Final Assignment

(Option D)

Assessing spatial and temporal patterns of drought variability and changing trend in Northeast China using the Standardized Precipitation Index

Summary

In my topic, the spatiotemporal variability of droughts was analyzed based on monthly precipitation data, from September 1960 to October 2010, in 95 rain gages distributed uniformly over NEC. The drought events were characterized by means of the multi-dimensional Standardized Precipitation Index (SPI). Results indicate that, droughts in most areas of NEC showed a significant increase during last 50 years.

Furthermore, the CMIP3 multi-model datasets during 1961-2060 for IPCC SRES A1B, A2 and B1 climate change scenarios were utilized to calculate which should be adequate to capture the spatial and temporal variations of drought and its response to climate change over NEC. Under the three climate-change scenarios, the period of the early 30 years during 2011~2060 would probably suffer many droughts, and the A2 scenario with heavy emissions should pay for more severe drought events than others. Overall, a comforted decrease of drought severity would response to future climate change in NEC; however, a big magnitude of drought severity will increase locally, which would likely to be an indicator of some extreme and mega-droughts.

Dr. LU Hongjian
Senior Engineer
Information Center of the Ministry of Water Resources, People's Republic of China
Beijing, China

luhj@mwr.gov.cn

1. Introduction

Droughts are slow-onset and recurrent natural disasters always accompanying the long river of human history, and have been more and more highly concerned by various departments of society (e.g., agriculture, environment, water resources management) during last few decades. Droughts are creeping phenomena and occur in virtually all climate zones, such as high as well as low rainfall areas and are mostly related to the reduction in the amount of precipitation received over an extended period of time, a season or several years. It is not surprised that approximately half of the earth's terrain are susceptible to droughts; more importantly, almost all the major agricultural lands are located in these drought-prone areas. Among all the natural hazards during twentieth century, droughts resulted in extensive impacts on human society spanning a variety of sectors, e.g., agriculture, industry, water supply, and so on. In the past three decades, many large-scale severe and extreme droughts, inevitably costing insidious social and economic losses, had frequently visited Europe, Africa, Asia, Australia and American continent.

The Northeast China region (hereafter named as NEC) is located in the eastern edge of Eurasia continent with relative high latitude and belongs to a temperate zone with a prevailing monsoon climate. Adequate rain and heat simultaneously nourishing crops during the growing season (conventionally from May to September) are favorable to agriculture cultivation in NEC. Therefore, it has become one of the hugest commodity granaries in China, and its productivity could be more potentially stimulated under suitable environmental conditions. However, uneven distributions of precipitation in spatial and temporal scales as well as the rapid development of national economics in NEC caused acute conflicts between arising water demand and available water supply. And the latter is mainly recharged by precipitation resulting from atmospheric vapor. Particularly, NEC has been more frequently struck by droughts since the mid-1990s, for instance, an unprecedented drought, beginning in 1999 and continuously extending to 2001, had resulted in threats to the booming of regional economy and quality improvement of people's bread in this area.

2. Study area

The NEC (38°43′ N~53°33′ N, 117°16′ E~135°2′ E), just as its name implying, a vast region with a total geographical area of about 124.3×10^4 km^2 located in Northeast China (Fig.1), generally comprises Liaoning Province, Jilin Province, Heilongjiang Province and the east portion of Inner Mongolia prefecture. The Songnen plain, central area of NEC is surrounded by mountains from all aspects except for the south, bringing up a Horseshoe geomorphology. The elevation ranges from a minimum of 0 m to a maximum of 2479 m (Fig.1). The Greater Khingan with an elevation of about 1000 m stands in northwest NEC while a series of mountains and ridges (i.e., Changbai Mountain, Dahei Moutain, Wanda Mountain, Hada Ridge, Zhangguangcai Ridge and Laoye Ridge) set in east NEC. Zonal vegetation types contain cold-temperate coniferous forest covering the north of the Greater Khingan, temperate mixed conifer and broad-leaved forest thriving in east NEC, and temperate semi-humid forest steppe adorning some plain districts.

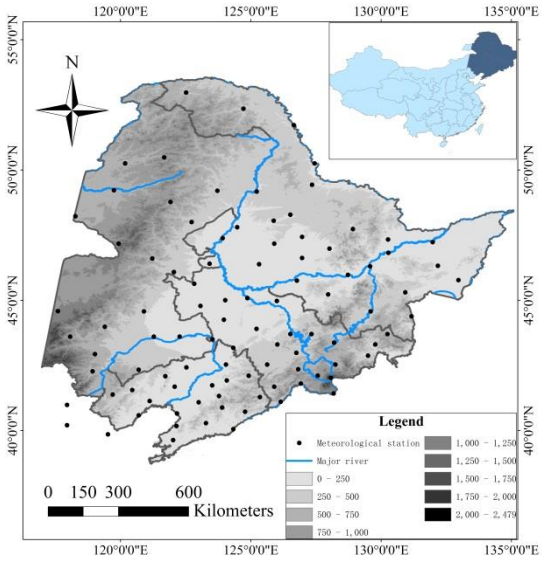

Figure1. Locations of meteorological stations in NEC and its DEM

The mean annual precipitation in NEC is 489 mm, successively decreasing from southeast area to the northwest area, which is 635 mm, 481 mm, and 355 mm, respectively, in the east, central, and west regions. Heilongjiang River, Songhua River, Wusuli River, Nenjiang River, Tumen River and Yalu River are the major waterlines inlaying across NEC. Since the surface runoff dominantly depending on the

spatio-temporal distribution of precipitation, the total runoff volume progressively diminishes from southeast to northwest while the annual runoff average can reach up to 500-600 mm in some areas like Tonghua City and the Jiaohe River.

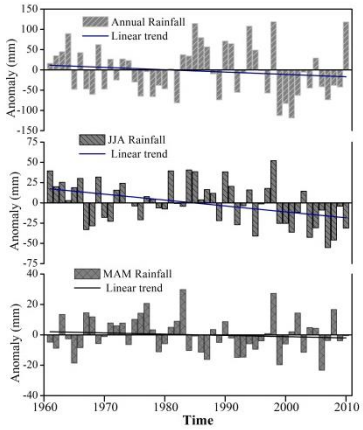

Figure2. Temporal variability of annual and seasonal precipitation in NEC during 1960~2010

3. Methodology to SPI calculation

The Standardized Precipitation Index (SPI) is a drought index based upon the probability distribution of a long-term precipitation series (McKee et al., 1993). The calculation of SPI is presented as follows (more details from http://ccc.atmos.colostate.edu/pub/spi.pdf): Firstly, it is fitted with a probability density function to the frequency distribution of precipitation summed over the time scale of interest. This is performed separately for each month (or any other temporal basis of the raw precipitation time series) and for each location in space. Each probability density function is then transformed into a standardized normal distribution.

The gamma distribution is defined by its probability density function is

$$g(x) = \frac{1}{\beta^{\alpha}\Gamma(\alpha)} x^{\alpha-1} e^{-x/\beta} (x > 0) \qquad (1)$$

Where x is the precipitation amount of the desired time step, α is the shape parameter, β the scale parameter, and the gamma function is expressed as

$$\Gamma(\alpha) = \int_0^{\infty} x^{\alpha-1} e^{-x} d_x \qquad (2)$$

Fitting the distribution to the data requires that α and β be estimated. Edwards and

McKee (1997) suggested a method for estimating these parameters using the approximation of maximum likelihood as follows:

$$\hat{\alpha} = \frac{1+\sqrt{1+4A/3}}{4A}$$

$$\hat{\beta} = \frac{\bar{x}}{\hat{\alpha}} \qquad (3)$$

where

$$A = \ln(\bar{x}) - \frac{\sum \ln(x)}{n}$$

Where n is the total number of the precipitation records.

Then the cumulative probability of an observed precipitation event for the given month or any other time scale can be obtained by the following equation:

$$G(x) = \int_0^x g(x)d_x = \frac{1}{\hat{\beta}^{\alpha}\Gamma(\hat{\alpha})}\int_0^x x^{\alpha-1}e^{-x/\beta}d_x \qquad (4)$$

Letting $t = x/\hat{\beta}$, the incomplete gamma function can be gained:

$$G(x) = \frac{1}{\Gamma(\hat{\alpha})}\int_0^x t^{\hat{\alpha}-1}e^{-t}d_t \qquad (5)$$

Considering the probability for a precipitation amount of zero (x = 0) during a week or a month for some arid and semi-arid climatic zones, the cumulative probability becomes:

$$H(x) = q + (1-q)G(x) \qquad (6)$$

Where q is the probability of a zero and is estimated by m/n, m is the number of zeros in precipitation records, and n is the length of the precipitation series. For larger time scales (like 3-, 6-, 12-, 24-month) the probability of monthly null precipitation is zero. So the errors in calculating the parameters α and β due to the monthly null precipitation does not affect the distribution at larger time scales.

The cumulative probability of the distribution for each value of precipitation is then transformed using equal probability to a normal distribution with a mean of zero and standard deviation of one, which is the value of the SPI. For a given cumulative probability H(x), the corresponding normal distribution probability can be estimated by using following equation (Edwards and McKee, 1997):

While $0 < H(x) \le 0.5$

$$Z = SPI = -(t - \frac{c_0 + c_1 t + c_2 t^2}{1 + d_1 t + d_2 t^2 + d_3 t^3}) \quad (7)$$

$$t = \sqrt{\ln\left[\frac{1}{H(x)^2}\right]}$$

While $0.5 < H(x) < 1$

$$Z = SPI = (t - \frac{c_0 + c_1 t + c_2 t^2}{1 + d_1 t + d_2 t^2 + d_3 t^3}) \quad (8)$$

$$t = \sqrt{\ln\left[\frac{1}{[1.0 - H(x)]^2}\right]}$$

Where c_0 = 2.515517; c_1 = 0.802853; c_2 = 0.010328; d_1 = 1.432788; d_2 = 0.189269; and d_3 = 0.001308.

Drought categories based on the SPI methodology according to Mckee et al. (1993) are defined and listed in Table 1, which are provided by the National Drought Mitigation Center (NDMC, http://drought.unl.edu), and its symmetry properties allows the detections both for drought and wetness episodes.

Table 1 Wet and drought classifications according to the SPI values

SPI value	Category	Probability %
2.00 or more	Extremely wet	2.3
1.50 to1.99	Severely wet	4.4
1.00 to1.49	Moderately wet	9.2
0 to 0.99	Mildly wet	34.1
0 to −0.99	Mild drought	34.1
−1.00 to −1.49	Moderate drought	9.2
−1.50 to −1.99	Severe drought	4.4
−2.00 or less	Extreme drought	2.3

4. Data and methods of analysis

Rainfall data sets: Daily precipitation of 95 rain gauged stations in NEC from China Meteorological Administration (CMA, http://cdc.cma.gov.cn/) were utilized to calculate historical SPI series at 3, 6, 12, 24-month scales (signaled by SPI3, SPI6, SPI12 and SPI24, respectively) during 1961-2010. Then the gridded monthly precipitation of CMIP3 multi-model output for IPCC A1B, A2 and B1sociceconomic scenarios, downscaled by National Climate Center (NCC, http://ncc.cma.gov.cn/cn/) and extracted for NEC, were used to derive the simulated droughts by calculating the

SPI3 and SPI12 during two periods, i.e. 1961-2010 and 2011-2060. The statistical tests (Kolgomorov-Smirnov (K-S) and Chi-Square tests) show that rainfall in NEC follows a gamma distribution.

Mann-Kendall test: The nonparametric Kendall's test recommended by World Meteorological Organization and more suitable for non-normal distribution had been widely adopted in hydrometeorology and was used to testify the change trend of SPI at multiple scales in this study. A hypothesis test based upon the normalized Kendall's statistic Z, for a significance level of α, was applied to all variables for trend. To avoid serial correlation complications, Kendall's test was applied on a monthly basis. During the 50 years, for a significant level of $\alpha = 0.05$, each station statistics $|Z| \leq Z_{1-\alpha/2} = 1.96$, which means there is no remarkable change trend. As a smaller SPI indicated a drier situation, the positive and negative values of Z_s indicate the decreasing and increasing trends of drought, respectively.

Empirical Orthogonal Function (EOF): EOF analysis can reveal the major characteristics of spatial variations of a large set of correlated variables. It is a statistical technique that linearly transforms a primitive set of variables to a substantially smaller set of uncorrelated variables on behalf of the most critical information of the original set of variables. Fundamentally speaking, the EOF analysis aims to reduce the dimensionality of the primitive set of variables, which will give birth to a much smaller set of uncorrelated variables to understand and deal with the spatial variability better.

5. Results and analysis

5.1 Detection and trend of historical droughts

As illustrated in Fig.2, three major drought episodes can be extracted from the regionally averaged SPI series during 1961~2010, viz., the periods of late 1960s, from mid-late 1970s to early 1980s and from late 1990s to 2000s. Particularly, the third one with prolonged duration and heavier severity was the most serious episode. Effects of time scales of SPI series on drought characteristics obviously distinguished the different impacts of precipitation deficiency on a variety of water availability. The

SPI3 and SPI6 felicitously characterized short-term moisture deficit and seasonal droughts (e.g., agricultural drought during crop growing season), which usually occurred frequently but persisted in a little soon. In contrast, long-range droughts in NEC appropriately signaled by SPI12 and SPI24 lasted a prolonged period but came not so often. Therefore, major drought/wetness episodes can be identified by the SPI at 24-month or larger time steps due to its high temporal variability.

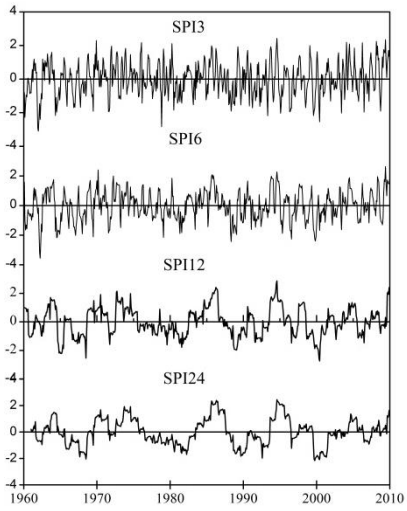

Figure3. Dry and wet episodes derived from SPI at different time steps in Shenyang station

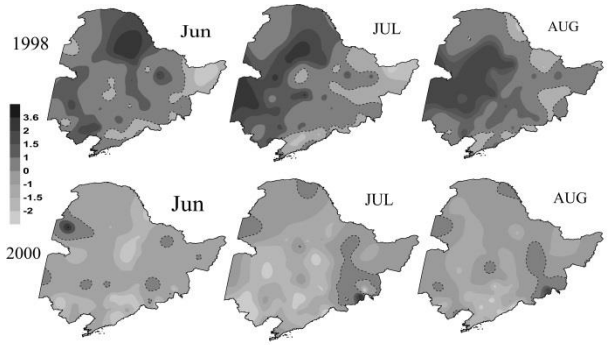

Figure4. Spatial patterns of drought and wetness severity characterized by SPI3 in typical years

Trend detected by the Mann-Kendall test indicated that drought severity had intensified during last 50 years in most areas over NEC, and impacts of time scale on change trends were conspicuous (Fig.5). At 3, 6, 12 and 24-month scales, there were 13, 28, 60 and 62 meteorological stations, respectively, where drought conditions showed a significant increasing trend at or more 95% confidence level. It was obviously noted that most stations in south NEC suffered drying trend during last 50 years at all timescales, cause of which was undoubtedly due to decreased precipitation.

However, drying trend became more widespread to central and eastern areas of NEC as time steps moving to 12 and 24 months, that may be attributed to inter-annual and inter-decade fluctuations of precipitation structure and changed frequency of extreme rain events.

Conversely, the numbers of stations showed a significant wetness trend on the four time scales were 24, 10, 7 and 9, respectively (Fig.5). In addition, because of wetting stations always scattering in areas of higher elevation and flourishing forest covers, it may be an important indicator that effects of elevation and vegetation be wonderful drought-mitigation contributors, especially during a shorter period (e.g., 3 or 6-month scale).

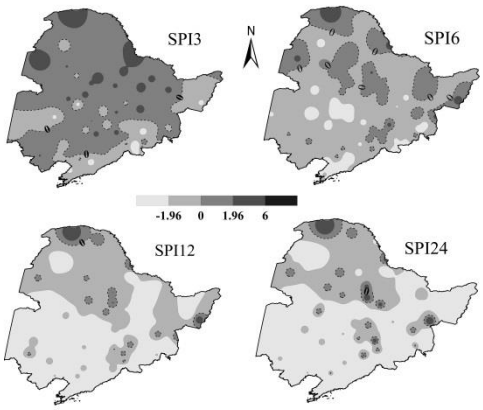

Figure5. Spatial distribution of the Z values detected by M-K

5.2 Spatial and temporal variations of historical droughts

Empirical Orthogonal Function (EOF) was used to determine the spatial patterns of drought characterized by SPI3 and SPI12 in NEC for last 50 years (Fig.5). The first EOF explained about 30% of the total variance, and the same symbol of the eigenvalue indicated an overall drying trend with a drought core in the Liao River basin in NEC. The second EOF explained about 11% of whole variance and showed the north-south pattern of drought severity with its center in southern part of NEC. On the other hand, the third EOF showed an east-west pattern with its highest severity in the western part of NEC while the fourth EOF captured a complex north-central-south

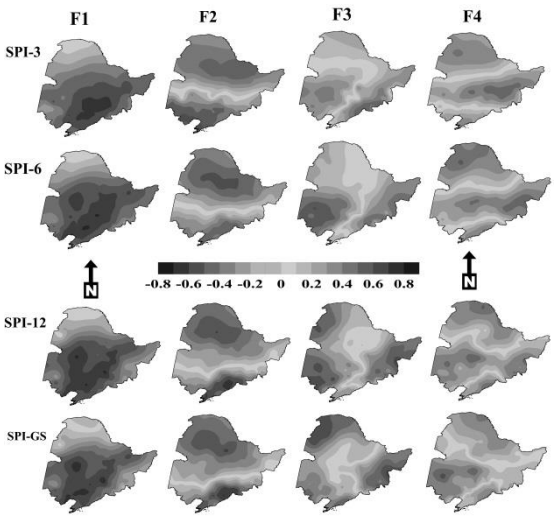

Figure6. The four major (F1, F2, F3 and F4, respectively) loading spatial patterns of drought severity on different scales across NEC

Table2

PCs no.	SPI3		SPI6		SPI12		SPI24	
	Total	Cumulative %	Total	Cumulative %	Total	Cumulative %	Total	Cumulative %
1	30.58	31.21	28.86	29.46	26.30	26.84	28.95	29.54
2	11.20	42.63	11.00	40.65	11.54	38.62	12.20	41.99
3	7.03	49.80	7.35	48.15	8.70	47.49	9.88	52.07
4	4.62	54.51	5.00	53.22	5.29	52.89	5.16	57.34
5	2.77	57.34	2.92	56.19	3.70	56.67	4.26	61.68
6	2.72	60.11	2.90	59.15	3.41	60.14	3.73	65.49
7	2.54	62.70	2.54	61.74	2.74	62.94	3.12	68.67
8	2.00	64.74	2.16	63.94	2.68	65.68	2.67	71.40
9	1.83	66.60	2.00	65.94	2.33	68.06	2.59	74.04
10	1.68	68.32	1.89	67.86	2.08	70.18	2.25	76.33
11	1.45	69.80	1.56	69.46	1.89	72.11	1.96	78.33
12	1.35	71.18	1.41	70.89	1.76	73.91	1.89	80.26
13	1.21	72.41	1.25	72.17	1.55	75.49	1.68	81.97
14	1.05	73.49	1.15	73.34	1.47	76.99	1.49	83.49
15			1.09	74.46	1.31	78.32	1.42	84.93
16			1.06	75.54	1.27	79.61	1.33	86.29
17			1.01	76.57	1.25	80.89	1.23	87.55
18					1.14	82.05	1.09	88.66
19					1.04	83.11		

pattern. The changing rates of drought severity in the third and fourth EOFs were steeper than those of the first and second EOFs; moreover, impacts of timescales on spatial patterns of drought severity were significant, especially for the third and fourth EOFs.

5.3 Spatio-temporal patterns of droughts under climate change

It is found that drought statuses of A2 and A1B scenarios would be much severer than B1 scenario after compared with each other; particularly, the A2 scenario with heavy emission would have to wait for an extended drought period in 2040s. Since the SPI is also significant in detecting wetting episodes, much attention should be paid on higher flood risk during the period of 2050-2060 especially for A2 and A1B scenarios.

The PC1 demonstrates the temporal trends of regional dryness/wetness, i.e., for A1B scenario, droughts would not have frequently occurred until 2040s except for a short interlude of wetness about in 2020; A2 scenario would own three major episodes, whose abrupt points can be detect in the years of 2020, 2033 and 2045, respectively; yet, for B1 scenario, besides a few droughts shared in 2050s, the years before 2020 would bear most of the droughts in the coming five decades.

It is particularly noteworthy that considerable wetness even strong floods would plague in NEC in 2050s under both A2 and A1B scenarios, which may be primarily resulted from the relative abundance of increasing precipitation caused by global warming. In addition, temporal transition points of PC2 and PC3 are always consistent with that of PC1, suggesting that dryness or wetness conditions at a local scale would simultaneously change with that at regional scale, and this is because they are all and only controlled by the changed regime of precipitation.

5.4 Impacts of climate change on drought severity

Because of the uncertainty of projected precipitation from GCMs, characteristics (e.g., duration and severity) of a drought event for a short period would not be accurately predicted. Thus, the cumulative drought severity (defined as the sum of the absolute values of SPI less than -1 within a drought event) of the period of 2011-2060 was adopted to subtract that of the period of 1961-2010, results showing different decreasing magnitudes of the A1B, A2 and B1 scenarios, i.e., 3.4%, 6.1% and 5.3%,

respectively. Regionally speaking, that would be a comforted surprise to the limited water resources in NEC, and would reduce some pressures from drying trend in a sense.

However, impacts of climate change on the overall drought severity will be significantly different from one grid to another; in other words, spatial variations of changed drought severity would split the whole NEC into many sub-districts. Locally, the southwestern and northern horns of NEC, the central and eastern parts of Heilongjiang Province and the southeast part of Jilin Province will probably suffer many large-scale droughts caused by increasing frequency of extremely low rain events on the condition of climate change.

6. Discussions

Drought is a normal part of the climate just like a potluck in any region due to the spatiotemporal heterogeneity of precipitation structure. During last five decades, the precipitation regime in the south of NEC changed significantly, for instance; annual and summer precipitation showed a significant decrease but intensity of rainfall and frequency of extreme rain events rose up. Because of based on the probability distribution of precipitation for a suitable period (no shorter than 30 years), the SPI indices could detect characteristics and trends of drought induced by the deficiency of precipitation. Regionally speaking, drought severity in NEC was aggravated since 1961, while declining from south to north. Temporal variation of drought was completely consistent with inter-annual or inter-decade variations of precipitation and spatial patterns of drought mainly depended on spatial heterogeneity of precipitation structure as well as its timescales, thus making out precipitation regime was the dominating driver of droughts in NEC during last 50 years.

Under different climate change scenarios (A1B, A2 and B1), the first 30 years of the period 2011-2060 will be likely to share most of the droughts resulted from precipitation deficit, and the A2 scenario with the heaviest emission should pay for the most serious drought condition, that is coincidentally consistent with the results projected by the ECHAM5/MPI-OM climate model; besides, the Liao River basin and the south part of Songhua River basin were mentioned to be the drought heart of NEC in next 50 years.

On the circumstance of global warming, a significant increase of annual

precipitation caused by the intensification of the water cycle would indeed happen to the whole NEC region, where overall drought severity would reduce to a certain extent. Nonetheless, drought severity (here signaled by SPI12) will drastically rise up in some local areas, which would probably result in more inhomogeneous distribution of dryness and wetness and imply more comings of large scale extreme drought events in NEC during the forthcoming half century.

Except for precipitation deficit, temperature is also great importance of the development of a drought event, so the coupled effects of increasing temperature and changing precipitation structure would be likely to bring about much more extreme events. Therefore, ignoring the role of a temperature increase in a calculated drought index may lead to underestimation of the impacts of global warming on regional drought conditions and inaccurate assessment of drought risk in different socioeconomic scenarios.

7. Conclusions

It is obvious that drought phenomenon will create more vulnerable environment for the agricultural sector and water resources in NEC. The impacts would vary greatly with varying time steps. Base on all the contexts contained in the present study the following conclusions can be drawn. Drought in most areas in NEC showed a significant increase during last 50 years, and areal extent of moderate and extreme droughts become more widespread. The first three decades in future 50 years would probably suffer many droughts, and the A2 scenario with heavy emissions has to pay for many severer droughts than others.

A comforted decrease of drought severity would response to future climate change; however, a big magnitude of drought severity will increase locally, which would likely to be an indicator of some extreme and mega-droughts for some raged areas in NEC. The conclusions reached in this study can be a preliminary step toward addressing the issue to drought vulnerability in NEC and can guide for drought management strategies for mitigation purposes. Identifying regional vulnerabilities can lead to adjustment in practices in water-dependent sectors and can help decision-makers to take the drought into account from hazard perspective and include the concept of drought vulnerability into natural resource planning.

8. Main References

Guttman N B. 1999. Accepting the Standardized Precipitation Index: A calculation algorithm. Journal of the American Water Resource Association, 35(2): 311-322.

McKee T B, Doesken N J, and Kleist J. 1993. The relationship of drought frequency and duration to time scales. Proceedings of Eighth Conference on Applied Climatology, Anaheim, California, pp. 17-22.

Wilhite D A. Drought as a natural hazard:Concepts and definitions [A]. Wilhite D A. Drought: A Global Assessment [C]. London & New York: Routledge. 2000, 3-18.